Multidisciplinary ⋮ Rapid Review ⋮ Open Access Journal

Date of publication xxxx 00, 0000, date of current version xxxx 00, 0000.

Digital Object Identifier 10.1109/ACCESS.2017.Doi Number

Enhancing the Signal Power Symmetry for Optical Phase Conjugation Using Erbium-Doped-Fibre-Assisted Raman Amplification

Mingming Tan[1], Tu T. Nguyen[1], Paweł Rosa[2], Mohammad. A. Z. Al-Khateeb[1, 3], Tingting Zhang[1], and Andrew. D. Ellis[1]

[1]Aston Institute of Photonic Technologies, Aston University, B4 7ET, Birmingham, UK

[2] National Institute of Telecommunications, 04-894, Warsaw, Poland

[3] now with Infinera Pennsylvania, 7360 Windsor Dr, Allentown, PA 18106, USA

Corresponding author: Mingming Tan (e-mail: m.tan1@aston.ac.uk)

The work was funded by the EPSRC programme grant EP/S003436/1 (PHOS) and EU MSCA grant 748767 (SIMFREE). We thank P. Harper and L. Krzczanowicz for insightful discussions, Sterlite Technologies and Finisar for industrial support.

ABSTRACT We propose a novel dual-order backward-pumped distributed Raman amplification scheme assisted erbium-doped-fibre (EDF) providing nearly perfect signal power symmetry (>93% symmetry level) over two 50.4 km single mode fibre spans. Compared with conventional dual-order Raman schemes, this scheme only requires an additional short (25 cm) erbium-doped fibre to compensate the loss from the passive components between spans, significantly improving the overall link symmetry. Unlike a conventional hybrid Raman/EDFA approach with separate amplifier modules, the proposed scheme offers cost savings by utilizing the Raman pumps to activate the erbium-doped fibre, avoiding the need for an EDF-designated pump. In an optical transmission system with four 50.4 km fibre spans, our novel Raman scheme presented in this paper enables mid-link optical phase conjugation (OPC) to compensate up to 37 dB of nonlinear Kerr inter-signal interference. This represents a 12 dB advantage in compensation over conventional dual-order Raman amplification. Our experimental and simulated results also demonstrate that the proposed configuration provides 7 dB nonlinear threshold enhancement in a 200 Gb/s DP-16QAM 200 km inline transmission system using a mid-link OPC, exceeding the enhancement observed with the conventional dual-order Raman scheme. Our simulation results also show that the optimum Q^2 factor using the proposed scheme outperforms the conventional schemes at 2000 km.

INDEX TERMS Optical amplifiers, optical fibre communication, phase conjugation, nonlinear optics

I. INTRODUCTION

Optical phase conjugation (OPC) has proved to be an efficient technique to compensate both linear (e.g. chromatic dispersion) and deterministic nonlinear (e.g. intra channel effects due to the Kerr nonlinearity) optical fibre impairments [1-13]. This technique could help exceed the "nonlinear Shannon limit" and significantly improve the maximum transmission distance or the system data capacity in a long-haul transmission system [10-16]. In a mid-link OPC system the transmission link parameters, such as the length of the transmission fibre, the chromatic dispersion slope, and more importantly the signal power profile along the fibre determine the efficiency of nonlinear impairment compensation [14-18]. In [11,15], the link was amplified mainly by EDFAs with a mid-link OPC, and the results show that the transmission reach was not significantly enhanced due to the lack of symmetrical signal power profiles before and after a mid-link OPC [17]. In contrast, distributed Raman amplification (DRA) can be a superior solution in terms of the transmission performance. Using DRA instead of EDFA can improve the signal-to-noise ratio (SNR) and provide a better balance between the ASE noise and the fibre nonlinearity, and consequently offers better transmission performance, with or without a mid-link OPC [15, 19]. Furthermore, a DRA link can be designed to maximise the signal power profile symmetry and consequently the nonlinearity compensation efficiency. Thus, the DRA not only provides a better performance without OPC, but also gives a large margin of performance (reach or data capacity) improvement when deploying an

This article has been accepted for publication in a future issue of this journal, but has not been fully edited. Content may change prior to final publication. Citation information: DOI 10.1109/ACCESS.2020.3044525, IEEE Access

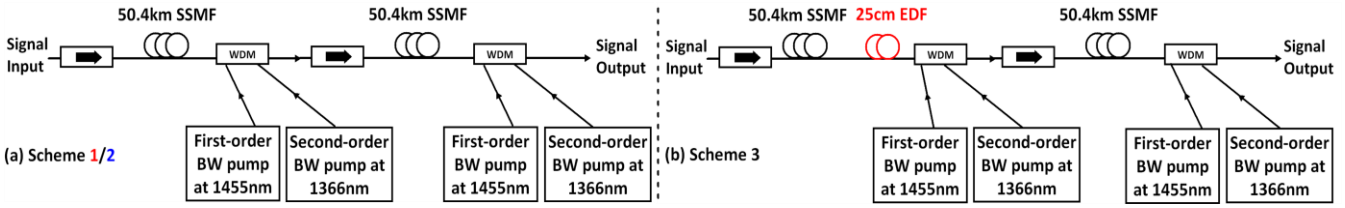

FIGURE 1. Scheme 1 and 2: Dual-order BW-propagated pumping DRA over 2x50.4 km SSMF (including two pump power settings). (b) Scheme 3: EDF-assisted dual-order BW-propagated pumping DRA over 2x50.4 km SSMF.

OPC to compensate a significant portion of the nonlinear interference accumulated across the long-haul transmission system. Previous studies showing significant benefit only focused on a single fibre span, where one may achieve signal power profile symmetry in different ways [18-20]. However, for a more practical multi-span link the attenuation from the passive components (mainly from the pump-signal combiners and the isolators) degrades the signal-power-profile symmetry. These point losses between spans play key roles in the overall multi-span signal power symmetry, which would have an impact on the nonlinearity compensation efficiency.

In this paper, we expand our previous work in which we proposed a novel distributed Raman amplification scheme to improves the symmetry of the signal power profile and therefore the efficiency of fibre nonlinearity compensation with a mid-link OPC [21]. The basis of this scheme was dual-order backward-pumped distributed Raman amplification assisted by erbium-doped fibre (EDF), which means the use of first- and second-order pumps in addition to a 25 cm erbium-doped fibre. This scheme allows an excellent (>93%) signal power symmetry over a two-span fibre link and enhances the fibre nonlinearity compensation efficiency. More importantly, the proposed scheme can also be applied to multiple fibre spans (>2 spans) without distorting the overall link symmetry. Unlike conventional hybrid EDFA/Raman amplifiers [22], the novelty of our approach lies in the Raman pump at 1455 nm also acting as the pump for the EDF simplifying the configuration. Here, we theoretically and experimentally demonstrate that, in the two-span link with mid-link OPC, using such EDF-assisted dual-order Raman amplification provides >12 dB more compensation than conventional dual-order Raman amplification in terms of nonlinear product power measurement. This scheme enables a minimum improvement of 7 dB in nonlinear threshold when transmitting a 200 Gb/s dual-polarisation (DP)-16QAM signal over 201.6 km (4×50.4 km) standard single mode fibre (SSMF) with a mid-link OPC, 1.5 dB more than conventional dual-order Raman amplification alone. We also show through simulation that the EDF-assisted scheme should give the best transmission performance at 2000 km.

II. MULTI-SPAN EDF-ASSISTED DUAL-ORDER DISTRIBUTED RAMAN AMPLIFICATION

In order to investigate the impact of multi-span DRA schemes on the nonlinearity compensation, we simulated the signal and noise power profiles of three dual-order DRA schemes with two 50.4 km standard single mode fibre (SSMF) spans and determined four-wave mixing (FWM) conversion efficiencies, and inline transmission performance in both experiments and simulations.

Scheme 1 was the conventional dual-order DRA with backward (BW)-propagated pumping which included both the first-order pump at 1455 nm and the second-order pump at 1366 nm [23] as shown in Fig. 1(a). The gain of the conventional dual-order DRA compensated only the loss from the SSMF, leaving the losses of the passive components (i.e. signal pump combiners, isolators, etc) uncompensated. In scheme 2, the setup was the same as scheme 1, but changing the pump-power of the first span compensated the loss due to fibre attenuation and the passive components between the two spans (~1.5 dB). That is the signal output power from the first SSMF was ~1.5 dB overpowered to account for this loss. In both cases, the gain in the second span (the last span in multi-span link) was set to compensate the attenuation from the fibre only. Finally, in scheme 3, in order to compensate the loss of passive components without sacrificing the overall symmetry of the two-span link, a 25 cm EDF (Fibrecore M-12(980/125)) was placed between the SSMF and the WDM coupler at the end of the first span as illustrated in Fig. 1(b).

This article has been accepted for publication in a future issue of this journal, but has not been fully edited. Content may change prior to final publication. Citation information: DOI 10.1109/ACCESS.2020.3044525, IEEE Access

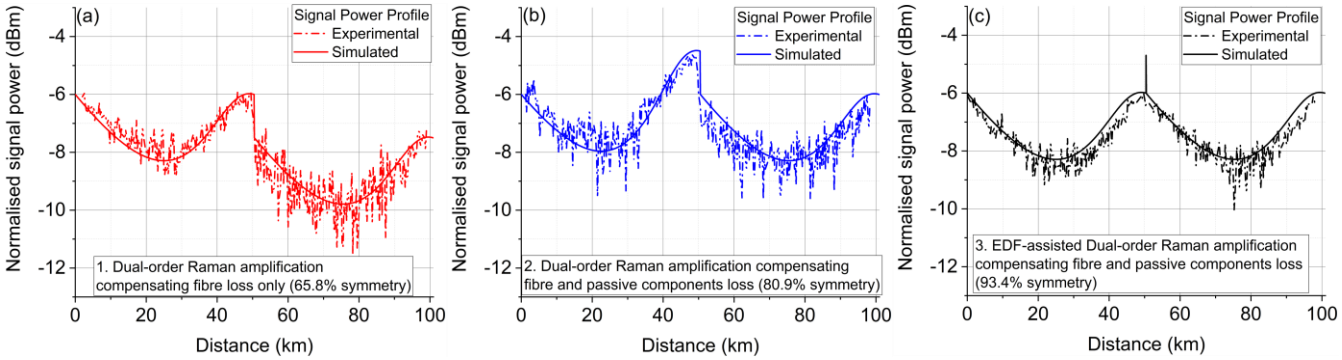

FIGURE 2. Experimentally measured and simulated signal power profiles along the fibre with three Raman amplification schemes; (a) 1. DRA compensating only the fibre loss. (b) 2. DRA compensating the fibre and the passive components' loss between the two spans. (c) 3. EDF-assisted DRA compensating fibre and the passive components' loss between the two spans.

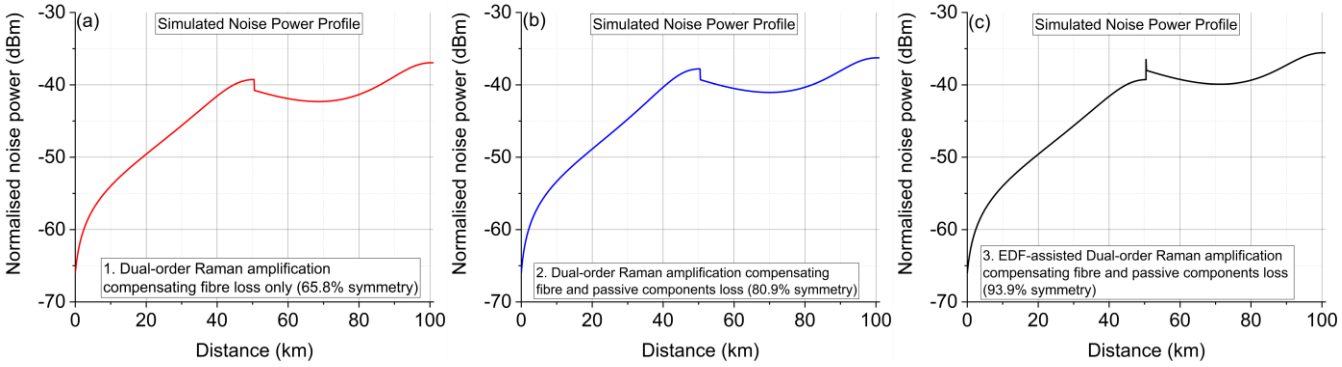

FIGURE 3. Simulated noise power profiles along the fibre with the three Raman amplification schemes

To simulate the DRA, we used an extended model [24] that takes into account: the first-order Raman gain (1455 nm); the Raman amplification of the first order pump by the second (1366 nm); the residual Raman gain induced by the second-order pump on the signal; Raman amplified double Rayleigh scattering (DRS); amplified spontaneous emission (ASE) noise for each signal; and all pump depletion processes. Simulations assumed that the Raman pumps at 1366 nm and 1455 nm were fully depolarised at room temperature, and that the bandwidths of both pumps and the signal were 200 GHz and 125 GHz respectively. The Raman gain coefficients and the attenuation factors for each frequency component were chosen with the respect to the standard Raman gain spectrum and the attenuation curve in SSMF shown in [24]. The values of the Rayleigh backscattering coefficients at the first-order pump at 1455 nm, second-order pump at 1366 nm and the signal channel were assumed to be 1×10^{-4}, 6.5×10^{-5} and 4.5×10^{-5} km^{-1}, respectively. The attenuation between the spans due to extra components (a WDM coupler and an isolator) were equal for all cases and assumed to be 1.5 dB. To simulate the EDF-assisted scheme 3 illustrated in Fig. 1(b), the attenuation and gain coefficient factors for all frequency components in 25 cm EDF placed at the end of the first span followed the specification sheet of the fibre Erbium Doped Fibre (Fibrecore M-12(980/125)) and were performed using a rate equation model [22, 25]. The step size was 0.1 km for SSMF and 1 cm for EDF.

For scheme 1, the pump power at 1366 nm was ~330 mW, higher than ~100 mW at 1455 nm, which provided 97% intra-span symmetry (as defined in [18]) a significant improvement over first-order pumping alone [20]. The pump powers compensated only the loss from the SSMF. Thus, in a two-span link, ~1.5 dB signal power degradation between two spans would be inevitable. The 1.5 dB signal power degradation was particularly crucial given that the signal power variation within single span was only ~3 dB, meaning that the overall link symmetry was seriously distorted giving only 65.8 % two-span symmetry. The symmetry level was calculated [18] based on the simulated signal power profile in Fig. 2(a). More importantly, the effect of such asymmetry in the signal launch power to the second/next span can be detrimental to the nonlinearity compensation efficiency in a mid-link OPC system [18]. This can be seen clearly from the signal power profiles (Fig. 2(a)) measured by Optical Time Domain Reflectometer (OTDR) with the isolator replaced by a WDM coupler with the same loss, and confirmed by the simulation. The simulated noise power profile along the fibre of this scheme is demonstrated in Fig. 3(a).

For scheme 2, the pump power in the first span was ~330 mW at 1366 nm and ~115 mW at 1455 nm, which is slightly higher than in scheme 1. The pump power in the second span remained the same as scheme 1 because it was

This article has been accepted for publication in a future issue of this journal, but has not been fully edited. Content may change prior to final publication. Citation information: DOI 10.1109/ACCESS.2020.3044525, IEEE Access

also set to compensate the attenuation from the fibre only. The slightly increased first-order pump power in the first span compensated the 1.5 dB loss from WDM coupler of the first span and the isolator of the second span. As the signal-power overcompensation in the first span (Fig. 2(b)) led to a signal power transparency, the improving the two-span symmetry of the signal power profile to 80.9 %. Fig. 3(b) shows the simulated noise power profile of scheme 2 in which the noise power at the output can be seen to be slightly higher than that in scheme 1. We attribute this to the higher gain from the first span.

In scheme 3, the pump power in the first span was ~330 mW at 1366 nm and ~108 mW at 1455 nm, while the pump power of the second span remained the same as scheme 1 and 2. The additional 1.5 dB EDF gain was generated by both pumps (primarily by 1455 nm, however then photon energy at 1366 nm would be partially transferred to 1455 nm) and therefore compensated the loss of passive components between the two spans. Unlike the conventional hybrid Raman/EDFA, the scheme used the Raman pumps at 1366/1455 nm to amplify the EDF instead of a dedicated 980 nm/1480 nm pump for EDF. Fig. 2(c) shows the measured and simulated signal power profiles along the fibre in the proposed configuration. This scheme enables a signal-power symmetry of 93.4 % over two 50.4 km spans, giving the highest overall symmetry for a 100 km link in comparison with 65.8% achieved in in scheme 1 and 80.9 % in scheme 2. The symmetry level of 93.4% over two 50.4 km spans is also comparable to the best symmetry level of 97% over a single 50.4 km span using an optimised dual-order Raman amplification shown in [20]. The reason for the slightly degraded symmetry of two spans is simply the accumulation of 97% asymmetry over two spans. Fig. 3(c) shows the noise power profile. Due to the gain provided by EDF, the noise power at the output is the highest among three schemes, as expected.

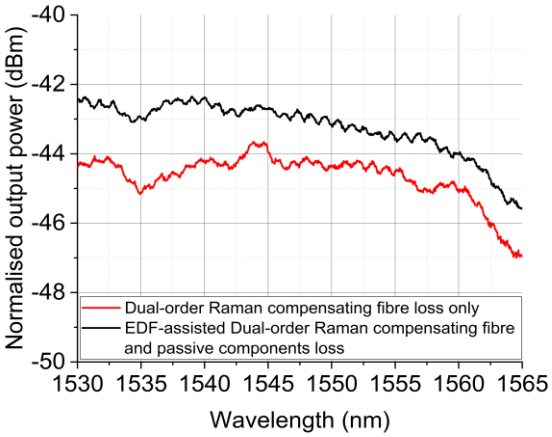

FIGURE 4. Measured output spectrum using the DRA compensating only the fibre loss and EDF-assisted DRA compensating both fibre and passive components loss.

Figure 4 shows experimentally measured output spectra using conventional dual-order DRA and EDF-assisted DRA over a single 50 km SSMF span (the first span in scheme 1 and 3 respectively). We can notice that with the same input (the ASE noise from an EDFA), the output spectra from both amplification schemes were similar to each other (other than ~1.5 dB higher gain from EDF-assisted scheme). This implies that there was no significant gain spectrum distortion due to the insertion of the 25 cm EDF fibre at the end of the first span.

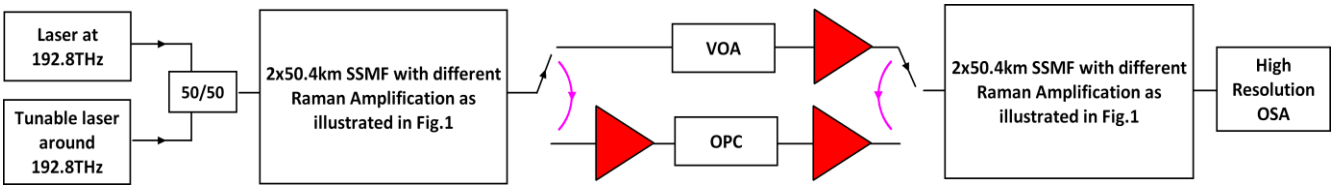

FIGURE 5. Experimental setup of nonlinear product power measurement with/without a mid-link OPC using different DRA schemes

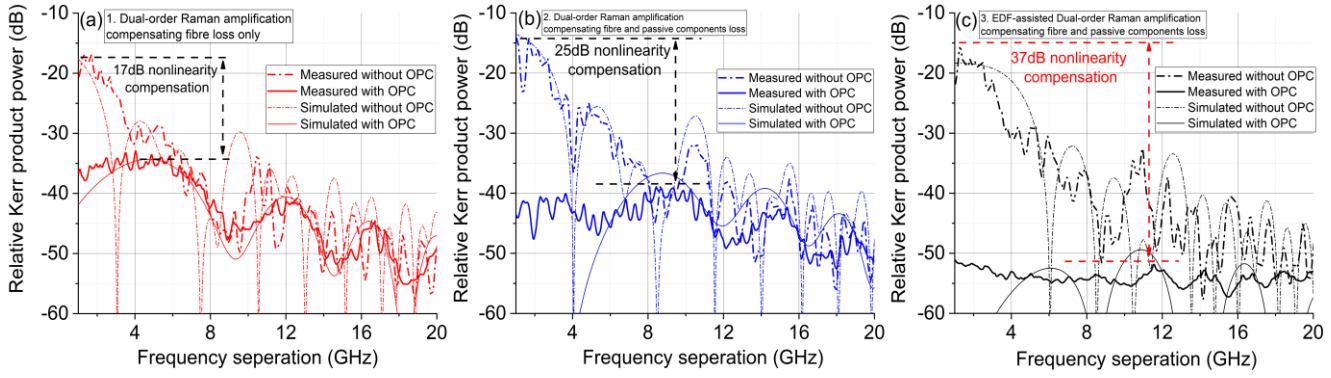

FIGURE 6. Experimentally measured and theoretically predicated nonlinear product frequency separation without/with a mid-link OPC using different DRA schemes

This article has been accepted for publication in a future issue of this journal, but has not been fully edited. Content may change prior to final publication. Citation information: DOI 10.1109/ACCESS.2020.3044525, IEEE Access

III. NONLINEAR PRODUCT POWER MEASUREMENT

Figure 5 shows a schematic diagram of the experiment used to evaluate the generation efficiency of nonlinear mixing products with and without a mid-link OPC using the three DRA schemes. Two 50.4 km Raman amplified SSMF spans were located before the OPC and another two spans after the OPC. The efficiency of the nonlinear product (degenerate four wave mixing) generation was established by launching two 3.5 dBm Continuous Wave (CW) lasers close to 192.8 THz (one fixed at 192.8 THz, the other one sweeping around 192.8 THz), and the generated nonlinear product was analysed with a 150 MHz resolution bandwidth optical spectrum analyser (OSA) [26]. For both paths, the input power to the second half of the 201.6 km link was adjusted with an EDFA. For the mid-link OPC path, we used an additional EDFA before OPC to pre-compensate the insertion loss of the OPC (~20 dB). The OPC used in this experiment was the dual-band, polarization insensitive, dual pump OPC reported in [26]. This experiment used only a single band.

The experimentally measured and theoretically predicted nonlinear product power is shown in Fig. 6 as a function of frequency separation of the two lasers using the three DRA schemes, where the calculation of the theoretically predicted curves also use the signal power profiles illustrated in Fig. 2 [26]. For the non-OPC path, the generated nonlinear Kerr product power for all the three DRA schemes was up to -16 dB in the strongly phase matched region (low frequency separation). However, because of the poor link symmetry caused by the signal power degradation between the first and second span, scheme 1 showed the least Kerr power reduction of only ~17 dB (comparing the two peaks of the nonlinear product power traces) with a mid-link OPC. Thanks to the improved link symmetry by the Raman pumps from the first span compensating the passive components' loss, enabled better Kerr product power compensation (~25 dB) to be achieved using scheme 2. The proposed scheme (scheme 3) used a 25 cm EDF to generate ~1.5 dB gain to compensate for the loss between spans, and therefore maintained excellent signal power symmetry simultaneously for both individual span and two spans link. This Raman scheme enabled the highest compensation (up to 37 dB) in nonlinear Kerr product power, which is comparable to the symmetry level of the single span in [20] whilst extending the result to a two-span configuration.

IV. TRANSMISSION RESULTS AND DISCUSSIONS

An inline coherent transmission experiment was performed for a 200 Gb/s DP-16QAM (32 GBaud, 256 Gbit/s line rate, 2^{15}-1 PRBS length, 0.1 roll-off factor) signal centred at 194.8 THz with three different DRA schemes with/without a mid-link OPC. After the link, the signal or the conjugated signal (centred at 194.65 THz) was amplified by an EDFA before being detected by a standard polarisation-diverse coherent receiver with a 100 GSa/s, 33 GHz real-time oscilloscope. The digital signal processing (DSP) at the receiver started with the resampling of the digital signal to two_samples-per-symbol. Then, the conventional procedure for data recovery in a typical coherent optical system was performed [27], including: chromatic dispersion (CD) compensation (using an inverse function of CD in the frequency domain), timing recovery and frequency offset correction (using a Gardner phase detector and a conventional Fourier-transform-based method, respectively), matched-filtering, an adaptive butterfly-structure equalizer (15 taps) to demultiplex the dual polarisation fields and compensate for PMD effects, carrier phase noise recovery (using the well-known blind phase search), down-sampling to one sample-per-symbol, and finally de-mapping QAM symbols into bits. Bit-error-rate (BER) measurement was performed by synchronizing and comparing the received bits with the transmitted bits. We used over 5×10^5 for the calculation, 7 using the inverse error function, of the binary-Q^2 factors shown in Fig.7.

We conducted a numerical simulation of the transmission performance of the DP-16QAM system while taking into account the signal and noise power profiles for each Raman scheme. The simulation setup is similar to the experimental one, using a random sequence of length 2^{16}-1 instead of the PRBS of length 2^{15}-1 adopted in the experiment. The system

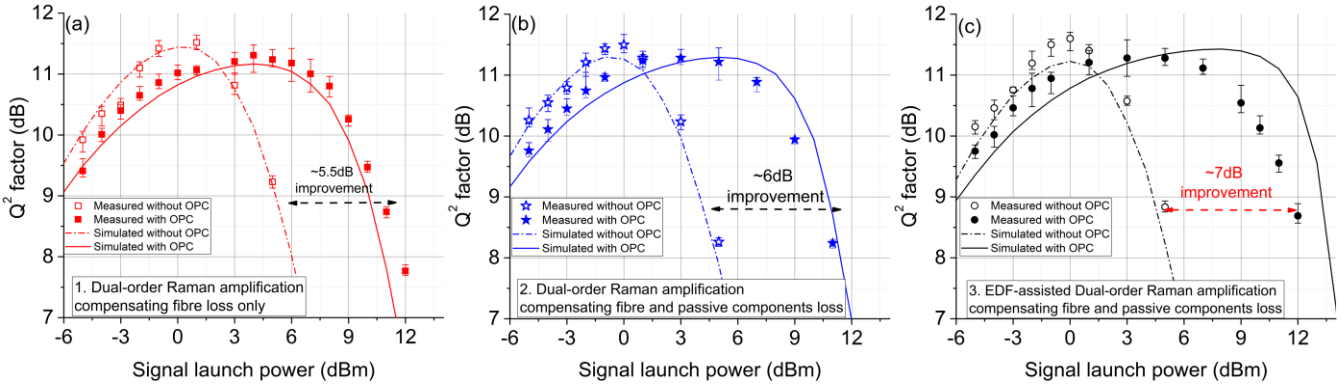

FIGURE 7. Experimentally measured and simulated Q^2 factors versus signal launch power in inline transmission systems with/without a mid-link OPC using different DRA schemes

This article has been accepted for publication in a future issue of this journal, but has not been fully edited. Content may change prior to final publication. Citation information: DOI 10.1109/ACCESS.2020.3044525, IEEE Access

was simulated by solving the coupled nonlinear Schrödinger equations (Manakov equations) using the well-known split-step Fourier method [28] with a step size of 0.1 km and the simulated signal power profiles shown in Fig. 3(a). Other key fibre parameters included the nonlinearity coefficient (1.3 /W/km) and dispersion (16 ps/nm/km). The Raman noise was modelled as Gaussian noise, which was added to the signal after each step (0.1 km), following the simulated noise profiles shown in Fig. 3(b). We used the same trend of the signal and noise power for all signal launch powers, for simplicity. The additional noise from EDFAs implemented in the experiments at the transmitter, the OPC setup and the receiver were taken into account in the simulations (ASE noise power density for each EDFA was approximately -140 dBm/Hz). The DSP adopted in the simulation was similar to the one used in the experiment.

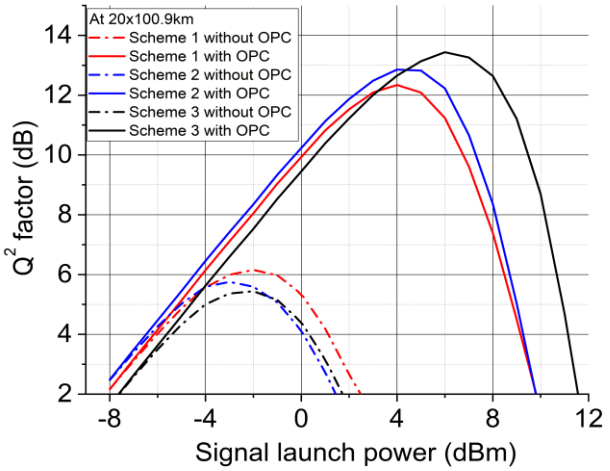

FIGURE 8. Simulated Q^2 factor versus signal launch power with/without OPC at ~2000km.

Figure 7 shows experimentally measured and simulated Q^2 factors versus signal launch power using the three DRA schemes over four 50.4 km spans of SSMF with/without a mid-link OPC. The proposed EDF-assisted scheme shows a maximum improvement of 7 dB in the nonlinear regime exceeding the improvement observed for the conventional DRA schemes 1 and 2 (by 1.5 dB and 1 dB), respectively. The slight difference between the experimental results and the simulation in Fig. 7(c) for EDF-assisted scheme was mainly because of a signal-power profile mismatch at high input signal power, as the pump depletion could lead to the changes in both the Raman and EDF gain. A precise power monitoring system would be required to help achieve more accurate results in particular for highly symmetrical link [20]. It has been established that this is due to the nearly perfect signal power symmetry (>93% symmetry) from the EDF-generated gain compensating the loss between two spans. As the total transmission distance was only ~201.6 km, the noise from the OPC/additional EDFA dominated the noise from the Raman-amplified link. This obscured the net Q^2 factor benefit expected from the nonlinearity compensation from the mid-link OPC and in fact resulted in the small reduction in optimum Q^2 factor with mid-link OPC [20].

Figure 8 shows simulated transmission performances at 2000 km using the three schemes. As the length of the link is ~2000 km and consequently the accumulated noise from the link (Raman-amplified spans) is dominant compared with the OPC noise, the benefit of the Q^2 factor can be revealed for long-haul transmission systems with a mid-link OPC. The Q^2 factor using scheme 3 is 0.6 dB and 1.1 dB better than scheme 2 and scheme 1, respectively. Therefore, using the symmetrical EDF-assisted Raman link can improve the fibre nonlinearity compensation efficiency in a mid-link OPC system.

V. CONCLUSIONS

We propose a novel dual-order distributed Raman amplification technique assisted by a short erbium-doped-fibre, which can improve the nonlinearity compensation efficiency over multi-span link when deploying a mid-link OPC. This technique can cost-effectively compensate the loss of passive components between the spans and therefore maximise the overall signal power symmetry up to 93% in realistic multi-fibre-span link. Unlike conventional hybrid Raman/EDFA amplification, our technique uses the Raman pump to amplify the erbium-doped fibre without a dedicated EDF pump. We demonstrate that, in the multi-span link with a mid-link OPC, using this scheme gives ~37 dB nonlinear product compensation. This is at least 12 dB higher than conventional dual-order Raman schemes. It has been also shown in both experiments and simulation that this novel Raman scheme gives a 7 dB enhancement of the nonlinear threshold in the 200 Gb/s DP-16QAM 200 km transmission system using a mid-link OPC, which is a minimum of 1 dB higher than conventional dual-order Raman schemes for both 200 and 2000 km links. Using the proposed amplification scheme with 2000 km SSMF link, we show that there is more than 0.6 dB improvement in the optimum Q^2 factor in simulation compared to alternative OPC schemes.

REFERENCES

[1] P. Minzioni *et al*., "Experimental Demonstration of Nonlinearity and Dispersion Compensation in an Embedded Link by Optical Phase Conjugation," *IEEE Photonics Technology Letters*, vol. 18, pp. 995-997, 2006.

[2] M. D. Pelusi, "WDM signal All-optical Precompensation of Kerr Nonlinearity in Dispersion-Managed Fibers," *IEEE Photonics Technology Letters*, vol. 25, 71-73, 2013.

[3] H. Hu *et al*., "Fiber nonlinearity mitigation of WDM-PDM QPSK/16-QAM signals using fiber-optic parametric amplifiers based multiple optical phase conjugations," *Opt. Express*, vol. 25, pp. 1618-1628, 2017.

[4] M. P. Yankov et al., "Probabilistic Shaping for the Optical Phase Conjugation Channel," *IEEE Journal of Selected Topics in Quantum Electronics*, vol. 27, pp. 1-16, 2021, Art no. 7700716, doi: 10.1109/JSTQE.2020.3024843.

[5] F. Da Ros *et al*., "Dual-polarization wavelength conversion of 16-QAM signals in a single silicon waveguide with a lateral p-i-n diode," *Photonics Research*, vol. 6, pp. B23-B29, 2018.

[6] P. Kaminski *et al*., "Improved nonlinearity compensation of OPC-aided EDFA-amplified transmission by enhanced dispersion

mapping," *2020 Conference on Lasers and Electro-Optics (CLEO)*, San Jose, CA, USA, 2020, pp. 1-2.

[7] S. Yoshima *et al*., "Mitigation of Nonlinear Effects on WDM QAM Signals Enabled by Optical Phase Conjugation with Efficient Bandwidth Utilization," *J. Lightwave Technol*., vol. 35, pp. 971-978, 2017.

[8] K. Solis-Trapala *et al*., "Optimized WDM Transmission Impairment Mitigation by Multiple Phase Conjugations," *J. Lightwave Technol*., vol. 34, pp. 431-440, 2016.

[9] S. Namiki *et al.*, "Multi-Channel Cascadable Parametric Signal Processing for Wavelength Conversion and Nonlinearity Compensation," *J. Lightwave Technol.*, vol. 35, pp. 815-823, 2017.

[10] T. Umkei *et al*., "Simultaenous nonlinearity mitigation in 92x180Gbit/s PDM-16QAM transmission over 3840km using PPLN-based guard-band-less optical phase conjugation," *Opt. Express*, vol. 24, no. 15, pp. 16945-16951, 2016.

[11] I. Sackey *et al*., "Kerr Nonlinearity Mitigation: Mid-link Spectral Inversion versus Digital Backpropagation in 5x28GBd PDM 16-QAM Signal Transmission," *J. Lightwave Technol*., vol. 33, pp. 1821-1827, 2015.

[12] I. Sackey *et al*., "Kerr Nonlinearity Mitigation: Mid-link Spectral Inversion versus Digital Backpropagation in 5x28GBd PDM 16-QAM Signal Transmission," *Opt. Express*, vol. 22, pp. 27381-27391, 2014.

[13] E. Bidaki, "A Raman-pumped Dispersion and Nonlinearity Compensating Fiber For Fiber Optic Communications," *IEEE Photonics Journal*, vol. 12, pp. 720017, 2020.

[14] A. D. Ellis *et al*., "Performance limits in optical communications due to fiber nonlinearity," *Adv. Opt. Photon.*, vol.9, pp.429-503, 2017.

[15] I. D. Phillips *et al*., "Exceeding the nonlinear-Shannon limit using Raman laser based amplification and optical phase conjugation," *OFC 2014*, San Francisco, CA, 2014, pp. 1-3.

[16] M. Al-Khateeb *et al*., "Experimental demonstration of 72% reach enhancement of 3.6Tbps optical transmission system using mid-link optical phase conjugation," *Opt. Express*, vol. 26, pp. 23960-23968, 2018.

[17] A. D. Ellis *et al*., "4 Tb/s Transmission Reach Enhancement Using 10 × 400 Gb/s Super-Channels and Polarization Insensitive Dual Band Optical Phase Conjugation," *J. Lightwave Technol.*, vol. 34, 1717-1723, 2016.

[18] P. Rosa *et al*., "Signal power asymmetry optimisation for optical phase conjugation using Raman amplification," *Opt. Express*, vol. 23, pp. 31772-31778, 2015.

[19] M. Tan *et al*., "Transmission performance improvement using random DFB fiber laser based Raman amplification and bidirectional second-order pumping," *Opt. Express*, vol. 24, no. 3, pp. 2215-2221, 2016.

[20] M. Al-Khateeb *et al*., "Combating Fiber Nonlinearity Using Dual-Order Raman Amplification and OPC," *IEEE Photonics Technology Letters*, vol. 31, no. 11, pp. 877-880, 2019.

[21] M. Tan, *et al.*, "Fiber Nonlinearity Compensation Using Erbium-Doped-Fiber-Assisted Dual-Order Raman Amplification," *2019 Conference on Lasers and Electro-Optics (CLEO)*, San Jose, CA, USA, 2019, pp. 1-2, doi: 10.1364/CLEO_SI.2019.SW3O.1.

[22] L. Lundberg *et al*., "Power consumption analysis of Hybrid EDFA/Raman amplifiers in long-haul transmission systems," *J. Lightwave Technol*., vol. 35, pp. 2132-2142, 2017.

[23] J.-C. Bouteiller *et al*., "Quasi-constant Signal Power Transmission," *Proc. ECOC*, Copenhagen, Demark, 2002, paper Symposium 3.4.

[24] P. Rosa *et al*., "Characterisation of random DFB Raman laser amplifier for WDM transmission," *Opt. Express*, vol. 23, pp. 28634–28639, 2015.

[25] Available at https://www.fibercore.com/product/erbium-doped-fiber-isogain

[26] M. A. Z. Al-Khateeb *et al.*, "Analysis of the nonlinear Kerr effects in optical transmission systems that deploy optical phase conjugation," *Opt. Express*, vol. 26, pp. 3145-3160, 2018.

[27] M. S. Faruk *et al*., "Digital Signal Processing for Coherent Transceivers Employing Multilevel Formats," *J. Lightwave Technol*., vol. 35, pp. 1125-1141, 2017.

[28] J. Zhang *et al*., "Digital Nonlinear Compensation Based on the Modified Logarithmic Step Size," *J. Lightwave Technol*., vol. 31, pp. 3546-3555, 2013